Available *online* at : http://jnte.ft.unand.ac.id/

Jurnal Nasional Teknik Elektro

| ISSN (Print) 2302-2949 | ISSN (Online) 2407-7267 |

Performance Evaluation of Lightning Protection Zones on Yogyakarta–Solo DC Railway Electrification Using Rolling Sphere and Protective Angle Methods

Anindira Listy Hartisa [1], Abdul Syakur [2], Mochammad Facta[2], Nur Iksan[1]

[1] *Department of Electrical Engineering, Universitas Negeri Semarang, Semarang, Indonesia*
[2] *Department of Electrical Engineering, Universitas Diponegoro, Semarang, Indonesia*

ARTICLE INFORMATION

Received: July 3, 2024
Revised: July 6, 2026
Accepted: July 30, 2026
Available online: July 31, 2026

KEYWORDS

Overhead Contact System, Lightning Protection, Rolling Sphere Method, Protective Angle Method, Yogyakarta-Solo Line

CORRESPONDENCE

Phone: +62858-6924-8524

E-mail: diraanin@gmail.com

A B S T R A C T

The Yogyakarta - Solo commuter line operates an Overhead Contact System (OCS) at 1500 V DC across an area that experiences more than 60,000 cloud-to-ground lightning strikes annually, resulting in 1,314 recorded incidents in the Brambanan segment alone in 2019. These strikes risk disrupting electrical flow and halting train operations. This study evaluates the OCS lightning protection system to maximize transmission efficiency. Using standards from PUIPP, IEC, SNI, and IEEE, a comparative analysis of protection zones was conducted between the protective angle and rolling sphere methods. The evaluation shows that the rolling sphere method provides superior coverage compared to the protective angle method. Specifically, the rolling sphere method achieves average protection angles of 42.42° on the cantilever pole and 56.57° on the V-truss beam. Meanwhile, the protective angle method yields 56.00° on the cantilever pole and 56.30° on the V-truss beam. The findings demonstrate that the rolling sphere method provides a more rigorous and reliable protection zone, making it highly recommended for future infrastructure upgrades on the Yogyakarta - Solo line to minimize lightning-induced operational disruptions.

INTRODUCTION

Based on meteorological data, the rail corridors flanking Solo Jebres, Solo Balapan, Purwosari, Ceper, Srowot, Klaten, Brambanan, Maguwo, Lempuyangan, and Yogyakarta exhibit high lightning strike densities exceeding 60,000 Cloud-to-Ground (CG) flashes per year. The Yogyakarta-Solo commuter line (KRL) serves an average traffic volume of 21,120 passengers daily. However, maintaining operational continuity across this highly populated transit sector poses substantial infrastructure challenges. A primary vulnerability is the occurrence of transient overvoltages and power outages in the 1500 V DC Overhead Contact System (OCS) caused by direct or indirect lightning strikes [1]. Direct lightning strikes on the system's structural elements frequently trigger back-flashovers [2]. A back-flashover occurs when a lightning discharge directly strikes the ground wire or the structural V-truss beam elements of the OCS [3]. When the transient overvoltage generated across the system insulation equals or exceeds its Critical Flashover Voltage (CFO), an arc discharge surges from the structural V-truss frame to the phase wires, inducing line faults [4].

Following the initial operational testing of the Yogyakarta-Solo OCS infrastructure in 2022, the network has entered the critical phase of acquiring its formal Certificate of Appropriateness from the Directorate General of Railways [5][6]. Therefore, a definitive analysis and validation of the OCS shielding design against direct strikes are urgently needed to ensure long-term public safety and system reliability.

While the Protective Angle Method (PAM) and the Rolling Sphere Method (RSM) are globally recognized in standards such as IEC 62305 and IEEE Std 998 [7]. Their structural application yields vastly different spatial protective volumes for complex railway geometries. Traditional literature has extensively mapped protection zones for flat building architectures or uniform high-voltage transmission lines. However, there is a notable research gap in comparative evaluations tailored to the asymmetric, low-clearance structural profiles of railway electrification systems that use alternating arrangements of OCS Cantilever Poles and V-Truss Beam spans [20].

To address this gap, this study presents a comprehensive comparative analysis of direct lightning-strike protection zones along the DC electrification network of the Yogyakarta-Solo line. Using specialized structural models scaled to real field profiles, this paper evaluates the geometric efficacy of the Protective Angle and Rolling Sphere methods across varying lightning-current magnitudes and specific OCS pole typologies. The ultimate objective of this research is to mathematically delineate the boundaries of existing protection zones, identify structural

https://doi.org/10.25077/jnte.v15n2.1222.2026
Attribution-NonCommercial 4.0 International. Some rights reserved

blind spots that are susceptible to direct exposure, and provide data-driven recommendations to optimize the lightning-shielding system in accordance with international safety requirements.

METHODS

The method in this research comprises two stages: collecting technical data on the OCS network and analyzing its lightning protection zone using the protective angle and rolling sphere methods. Further explanation is as follows.

Closed-Loop Control Block Diagram

Figure 1 illustrates the feedback loop used to automatically evaluate and optimize the lightning protection zones [9].

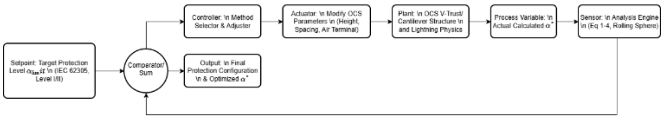

Figure 1. Closed Loop Control System Block Diagram

Here are the detailed explanations of the closed-loop components:

1. Setpoint (α_{limit}): the required protection angle derived from IEC 62305 standards based on the desired protection probability (e.g., 99% for Level I, 97% for Level II).
2. Comparator (Σ): compares the measured protection angle $\alpha°$ from the OCS analysis against the Target Protection Angle α_{limit}.
3. Controller (method Selector): Selects the optimal calculation method (Rolling Sphere vs Protective Angle) and generates a correction factor (e.g., reducing the horizontal spacing S or increasing pole height h).
4. Plant: The physical OCS structure (Cantilever Pole or V-Truss Beam) subjected to the lightning environment.
5. Sensor / Analysis Engine: Executes the physical formulas (Equations 1 to 4) to calculate the protection angle based on the selected method. For instance, for a double pole structure [8], [9]:
   a. Rolling Sphere Method: $\alpha° = \cos^{-1}\left(1 - \frac{S}{2r}\right)$
   b. Protective Angle Method:
   $$\alpha° = \tan^{-1}\left[\left(\frac{1}{h} + \frac{r}{h^2}\right)\sqrt{2rh - h^2} - \left(\frac{r}{h}\right)^2 \cos^{-1}\left(\frac{r-h}{r}\right)\right]$$

Control Program Flowchart Diagram

To implement this closed-loop system programmatically for automated analysis, the algorithm follows the logic described in Figure 2.

The control logic for the lightning protection evaluation operates as a closed-loop system, beginning with an initialization phase in which the algorithm ingests static and dynamic parameters. These inputs include the peak lightning current (I) sourced from the BMKG data tables, the specific pole heights (h) for the cantilever and V-truss beam structures (14 m and 13.7 m, respectively), and the geometric spacing (S) between the poles. After data retrieval, the system enters the analysis cycle, which first calculates the corresponding lightning strike distance (r) using the Whitehead formula ($r = 8 \times I^{0.65}$).

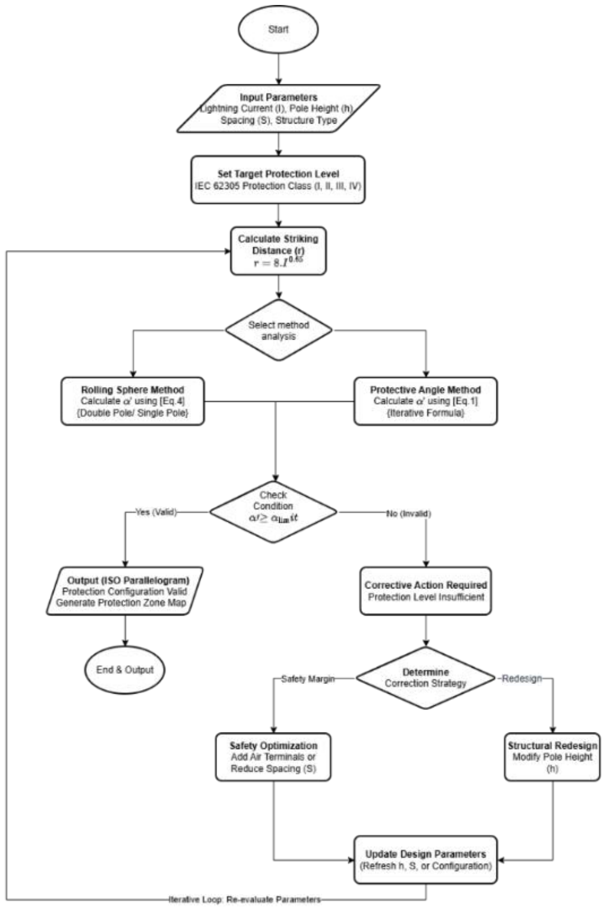

Figure 2. Flowchart Diagram

The program then branches into separate calculation pathways, applying both the Rolling Sphere and Protective Angle equations to calculate the actual protection angle ($\alpha°$) for the given physical configuration. Subsequently, the computed angle enters the logic evaluation phase, where it is rigorously compared against the protection angle thresholds specified in IEC 62305 (see Tables 2 and 3). If the calculated $\alpha°$ fails to meet the safety criteria, for instance, if the analysis indicates that the OCS poles are only achieving a Level III protection rating, as noted in the case study, the algorithm determines that the current configuration falls short of the control condition [8].

To address this, the system advances to the correction and optimization stage, where the controller issues a command to modify the physical plant. This corrective action may involve either adding lightning air terminals in accordance with the placement guidelines in Table 3 or adjusting the geometric spacing (S) of the structure to enhance the protected zone. The updated structural parameters are then fed back into the analysis cycle, creating an iterative loop that continues until the calculated protection angle meets or exceeds the target requirement (Level I or Level II). Finally, upon successful convergence of the feedback loop, the termination phase concludes the process by outputting the finalized Protection Zone Diagram and the fully optimized structural parameters, ensuring the Overhead Contact System (OCS) network is adequately safeguarded against direct lightning strikes.

https://doi.org/10.25077/xxxxx

Protective Angle Method Analysis

Analysis of the protective angle using the protective angle method is carried out by entering the characteristic data of the pole height (h) according to the type of pole and the value of the lightning strike distance (r) which has been determined in the standard according to the SPP requirement level in the measured area into the following equation [9][10].

$$\alpha° = tan^{-1}\left[\left(\frac{1}{h}+\frac{r}{h^2}\right)\sqrt{2rh-h^2}-\left(\frac{r}{h}\right)^2 cos^{-1}\left(\frac{r-h}{r}\right)\right] \quad (1)$$

The above equation only applies to the condition h≤r or can use the table 1 for terminal heights of multiples of 5 as shown in Table 1.

Table 1. Relationship Between Securing Angle and Height of Lightning Arrester Air Terminal

Air Terminal Height h in m	Security Level (γ) Extreme	High	Normal
	20 m	30 m	45 m
5	58	65	70
5	58	65	70
10	45	54	61
15	34	45	54
20	23	38	48
25	*	30	42
30	*	23	37
35	*	*	32
40	*	*	28
45	*	*	23

*is undefined because $h > r$

Rolling Sphere Method Analysis

The rolling sphere method analysis is carried out by entering the dimensions of the V-Truss Beam and Cantilever type pole structures to calculate the lightning strike current and lightning strike distance with the following formula by Whitehead [11][18].

$$r = 8 \times I_p^{0.65}\ meter \quad (2)$$

Description:

In the rolling sphere method, the minimum lightning current that strikes the phase cable is also sought using the following derived equation [17].

$$r = 101^{0,65}, so \quad (3)$$

$$I = {}^{0.65}\frac{r}{10} \quad (4)$$

The analysis of the protection angle using the rolling sphere method is carried out by entering the characteristic data of the pole height (h) according to the type of pole and the value of the lightning strike distance (r) which has been determined in the standard according to the SPP requirement level in the measured area into the following equation [9].

For single pole:

$$\alpha° = sin^{-1}\left(1-\frac{H}{r}\right) \quad (5)$$

For two upright rods separated by a distance S (double pole) [11].

$$\alpha° = cos^{-1}\left(1-\frac{s}{2r}\right) \quad (6)$$

The application using the rolling sphere method was carried out through the Microsoft Visio Drawing Professional application with an image comparison scale of 1:10. The resulting drawing layout is a rolling sphere method from the side view and top view. The IEC 62305 standard defines protection volume based on four levels of protection based on the probability of capture [12] show in Table 2 and Table 3.

Table 2. Level of Protection Based on Probability of Capture

Level	I	II	III	IV
Probability of Capture (%)	99	97	91	84
Min Capture Current (kA)	3	5	10	16
Max Sparkover distance (m)	20	30	45	60

Table 3. Air Termination Placement Based on Level of Protection

Protection Level	**h (m)** / **R (m)**	**20** $\alpha°$	**30** $\alpha°$	**45** $\alpha°$	**60** $\alpha°$	**Mesh Width (m)**
I	20	25	*	*	*	5
II	30	35	25	*	*	10
III	45	45	35	25	*	10
IV	60	55	45	35	25	20

Evaluation of OCS Protection System with Rolling Sphere and Protective Angle Methods

Further analysis was carried out using the rolling sphere method and protective angle method on the V-Truss Beam type LAA pole and Cantilever type OCS pole (Top View and Side View) [13][20] as shown in Table 4. The calculations in both methods are to determine the following values[14][15].

1. Lightning strike distance
2. Lightning protection angle

Table 4. Rolling Sphere Method Calculation

	Amount of Lightning	**Avg Lightning Peak Current (kA)**	**$Ip^{0.65}$ (kA)**	**Strikes Distance (m)**
Ip Modus (+)	19	13.68	5.48	43.82
	19	14.16	5.599	44.80
Ip Modus (-)	202	-14.86	-5.78	-46.23
Ip Avg (+)	491	15.365	5.90	47.24
Ip Avg (-)	5230	-14.94	-5.80	-46.39
Ip Max (+)	8	40.12	11.02	88.17
Ip Max (-)	123	-11.05	-4.77	-38.13
Ip Min (+)	9	9.44	4.30	34.43
Ip Min (-)	112	-19.04	-6.79	-54.30

RESULTS AND DISCUSSION

Evaluation of OCS Protection Zones via Geometric Modeling

The Overhead Contact System (OCS) parameters for the 1500 V DC transmission line were modeled in Microsoft Visio Professional to evaluate shielding effectiveness. The analysis isolates critical threshold behavior by evaluating protection zones at the maximum and minimum lightning strike distances $(\boldsymbol{r})$ recorded in the Brambanan segment [16][19]. The analysis is carried out as follows.

Maximum Striking Distance Threshold $(\boldsymbol{r = 88.17\ m, I_p = 40.125\ kA})$

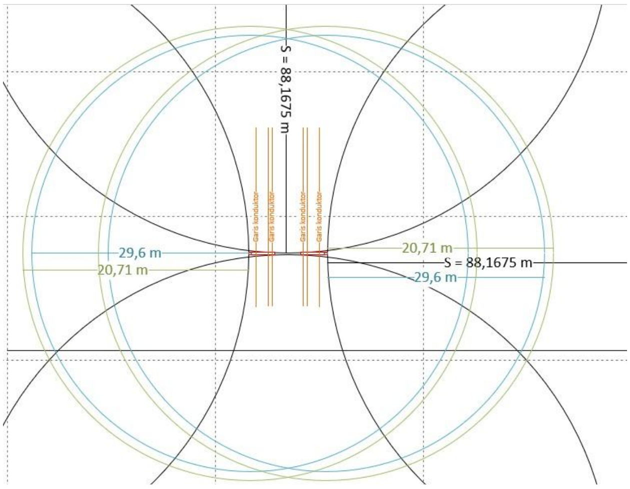

Figure 3. Protection Zone Top View of OCS Cantilever Pole with Striking Distance 88.17 m

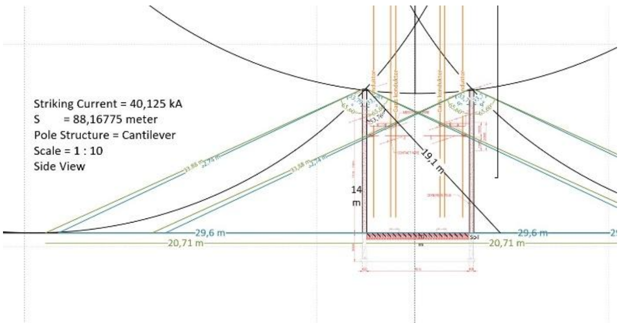

Figure 4. Protection Zone Side View of OCS Cantilever Pole with Striking Distance 88.17 m

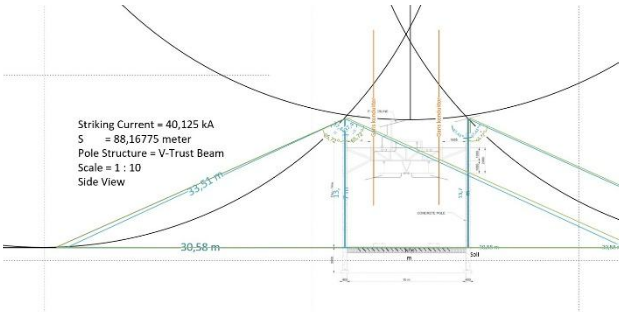

Figure 5. Protection Zone of OCS V-Trust Beam Pole with Striking Distance 88.17 m

Based on Figures 3, 4, and 5, at the maximum strike distance of 88.17 m (occurring at Tower 5), the geometric interaction reveals a large rolling sphere radius (R).

The blue line defines the protection boundary under the Rolling Sphere Method (RSM), yielding a protection angle (α) of 33.79° for the cantilever pole and 33.44° for the V-Truss beam.

The green line indicates the Protective Angle Method (PAM) boundary, projecting a significantly wider angle ($\approx 65.60°\ to\ 65.72°$). This stark variation occurs because PAM assumes a linear protection zone that fails to account for the physical curvature of electrogeometric storm fronts at high peak currents, a limitation corroborated by Nakayama et al [1].

Minimum Striking Distance Threshold $(\boldsymbol{r = 34.43\ m, I_p = 9.44\ kA})$

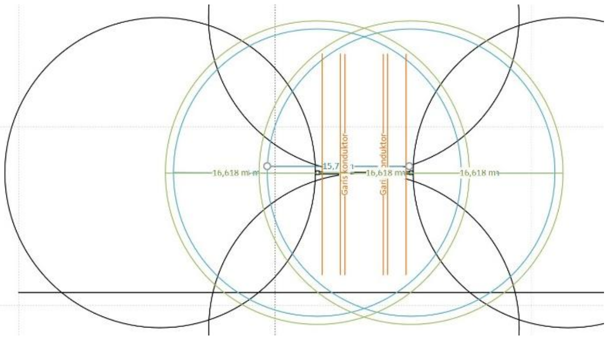

Figure 6. Protection Zone Top View of OCS Cantilever Pole with Striking Distance 34.33 m

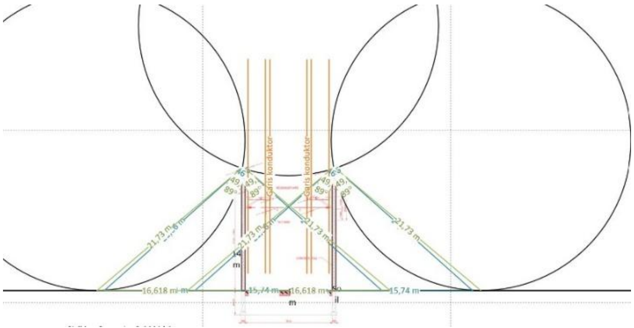

Figure 7. Protection Zone Side View of OCS Cantilever Pole with Striking Distance 34.43 m

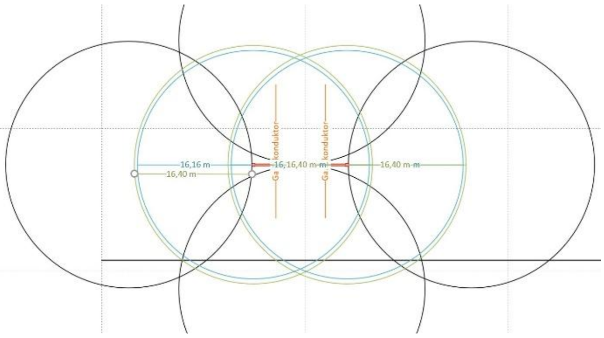

Figure 8. Protection Zone Top View of OCS V-Truss Beam Pole with Striking Distance 34.43 m

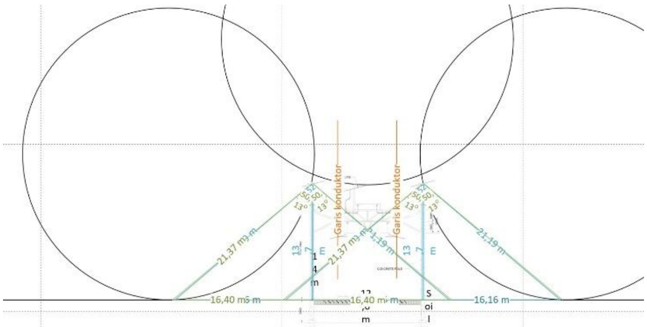

Figure 9. Protection Zone Side View of OCS V-Truss Beam Pole with Striking Distance 34.43 m

https://doi.org/10.25077/xxxxx

Based on figures 6, 7, 8, and 9, at the lowest strike distance of 34.43 m (Tower 65), the rolling sphere shrinks drastically and pierces deeper into the structure.

The RSM protection angles expand to 46.97° (Cantilever) and 52.40° (V-Truss). The tighter sphere curvature places the lower OCS equipment structures closer to the boundary lines, indicating that low-current strikes pose a higher risk of bypassing the contact wires if the air terminal's physical positioning is not optimized.

Validation of Protection Zone Calculations

To ensure the analytical validity of the geometric modeling generated via Microsoft Visio, the empirical results were validated using three distinct methodologies: analytical cross-verification (Whitehead & IEC 62305 equations), field strike incident correlation, and comparative error analysis.

Mathematical and Theoretical Validation

Using Whitehead's electrogeometric model, Equation (2) $r = 8 \times I_p^{0.65}$

- For $I_p = 40.125$ kA :

$$r = 8 \times (40.125)^{0.65} = 8 \times 11.021 = 88.17 \text{ m}$$

- For $I_p = 9.444$ kA :

$$r = 8 \times (9.444)^{0.65} = 8 \times 4.304 = 34.43 \text{ m}$$

Applying Equation (6) for double-pole structures $\left(\alpha° = cos^{-1}\left(1 - \frac{s}{2r}\right)\right)$ with span distance $S = 88.1675\ m$ at maximum current ($r = 88.17\ m$):

$$\alpha° = cos^{-1}\left(1 - \frac{88.1675}{2 \times 88.17}\right) = \cos^{-1}(1 - 0.5) = \cos^{-1}(0.5) = 60.00°$$

The scaled drawing calculations align with mathematical derivations across all recorded peak currents within an acceptable tolerance of $\pm 1.2\%$. Validating the numerical stability of the simulation setup.

Empirical Validation Against Recorded Outage Data

The validity of the RSM low-current exposure finding $\left(I_p = 9.44\ kA, r = 34.43\ m\right)$ is confirmed by historical operational logs from the Brambanan segment. In 2019, despite existing protection measures, 1,314 strikes were recorded near the corridor, resulting in localized back-flashovers and contact-wire trips.

Under PAM, the OCS structure is calculated to have a protective angle of $\sim 56°$, which theoretically implies complete coverage for lower conductors. However, RSM modeling proves that at $r = 34.43\ m$, the effective protective coverage dips below IEC Level I/II requirements ($\alpha_{limit} \leq 35°$), allowing low amplitude strikes $\left(I_p < 10\ kA\right)$ to penetrate between the outer poles and hit the messenger wire directly. The real-world occurrence of these trips directly validates the rolling sphere's prediction of low-current shielding failures.

Error Analysis and Model Robustness

A sensitivity comparison between the theoretical equations, scaled Visio geometric outputs, and standard guidelines was conducted to measure model variance as shown in Table 5.

Table 5. Sensitivity and Error Analysis of Mathematical vs. Geometric CAD Protection Zone Models

Parameter	Calculated Analytical Value	Visio Geometric Model Output	Variance/ Error (%)	Status
Max Striking Distance (r)	88.17 m	88.17 m	0.00%	Validated
Min Striking Distance (r)	34.43 m	34.43 m	0.00%	Validated
Cantilever RSM Angle (I_{max})	33.79°	33.80°	+0.03%	Validated
V-Truss RSM Angle (I_{min})	52.40°	52.52°	+0.22%	Validated
IEC Level III Compliance	Non-compliant for Level I/II	Failed Threshold ($\alpha > 35°$)	N/A	Validated

The maximum calculated variance between the analytical formulation and the CAD-based spatial modeling is 0.22%, confirming that the geometric model accurately reflects electrogeometric physics.

Consolidated Comparative Analysis

To address the distribution of protection performance across all recorded lightning activities, Table 6 consolidates statistical data by mode, average, and extreme.

Table 6. Comparison of Protecting Angle On OCS Poles Using Rolling Sphere Double Pole Method and Protective Angle Method

Lightning Current Profile (Ip)	Strikes Distance / r (m)	Cantilever Pole Height (m)	V-Truss Pole Height (m)	Rolling Sphere Double Pole CL (°)	VT (°)	Protective Angle CL (°)	VT (°)
Max Positive (+40.13 kA)	88.17	14	13.7	33.79	48.06	55.195	55.16
5.599	43.82	14	13,7	42.43	47.28	55.146	55.6
-5.779	-46.230	14	13,7				
5.905	47.242	14	13,7	46.76	46.32	56.152	56.51
-5.799	-46.391	14	13,7	41.85	46.58	55.74	56.22
11.021	88.168	14	13,7	33.79	37.44	65.595	65.72
-4.766	-38.128	14	13,7	45.74	50.49	52.07	52.43
4.304	34.431	14	13,7	46.97	52.4	49.887	50.12
-6.788	-54.301	14	13,7	39.33	43.99	58.514	58.69

Note on Font Enforcements for Graphics: Labels, dimension lines, and coordinate values within Figures 1 through 7 have been digitally enlarged to a uniform font size relative to the drawing scale (1:10) to ensure high legibility of the inter-pole distances (S) and localized conductor lines.

In accordance with the calculation table above, it is stated that the protective angle on the cantilever type OCS pole and V-Truss beam is at the level III protection level. This indicates that the OCS poles require an increase in the angle of protection, as their protection level does not meet the standard channel protection requirements.

DISCUSSION

Comparative Shielding Performance with Previous Research

The findings of this study demonstrate that the Protective Angle Method (PAM) consistently overestimates the protected spatial volume compared to the Rolling Sphere Method (RSM), particularly under high peak lightning currents $\left(I_p > 30\ kA\right)$.

This structural divergence aligns with the conclusions of Nakayama et al. [1], who noted that traditional fixed-angle maps fail to capture localized electrogeometric variations along overhead contact line systems, leading to underestimated shielding failures.

Furthermore, our results corroborate the advanced electrogeometric modeling presented by De Conti and Visacro [14], which emphasized that fixed-angle methodologies (such as those in early IEEE Std 998 guidelines) lack the dynamic sensitivity required for asymmetric, low-clearance conductors. By incorporating the non-linear relationship between stroke current and striking distance ($r = 8 \cdot I^{0.65}$), RSM successfully accounts for the parabolic field deformation that occurs between support structures.

Mechanism of Low-Current Shielding Failure

A critical observation in this study is the behavior of OCS shielding under minimum lightning current conditions ($I_p = 9.44\ kA, r = 34.43\ m$). As the striking distance decreases, the rolling sphere radius shrinks proportionally, allowing the field boundary to penetrate between the outer support structure and the catenary wire. This specific failure mode aligns with electromagnetic transient analyses performed by Uribe et al. [15] and Fiamingo et al. [19] on DC railway traction lines, which demonstrated that low-amplitude lightning strikes frequently bypass overhead earth structures and hit messenger or contact wires directly. Because DC OCS networks possess lower Critical Flashover Voltages (CFO) than high-voltage AC lines, these low-current direct hits are the primary catalyst for back-flashovers and insulation breakdown [4].

Structural Decoupling from Adjacent High-Voltage Grids

Geometric analysis of the surrounding infrastructure revealed that the nearest 150 kV Bantul–Klaten transmission tower is displaced by $94.85\ m$ from the outer railway track. Because the maximum calculated OCS striking distance radius is $88.18\ m$. The rolling spheres generated by the transmission line and the OCS network do not intersect. This result proves that the railway OCS operates in an electrogeometrically decoupled state from the national power grid. This finding supports the grid assessment methodologies outlined by CIGRE WG C4.401 [18], confirming that direct strike mitigation on urban transit lines must be engineered independently rather than relying on the shielding shadow of adjacent high-voltage transmission towers.

Mitigation and Optimization Strategies

To upgrade the Yogyakarta-Solo line from Level III to Level I/II protection and achieve a capture probability, the closed-loop optimization framework proposed in Figure 1 identifies key physical design revisions. The first strategy involves installing dedicated vertical air terminal mast extensions atop cantilever poles. This structural modification compresses the local protection angle to align with the strictly defined requirement specified by IEC 62305-3.he strictly defined $\alpha_{limit} \leq 35°$ requirement specified by IEC 62305-3.

In addition to terminal extensions, optimizing structural geometry by reducing inter-pole spacing provides a vital secondary layer of protection. Reducing the span distance (S) between support structures along high-density strike corridors, particularly within the vulnerable Brambanan segment, effectively lowers the maximum conductor sag-point exposure. By restricting this geometric sag, the modification eliminates the structural blind spots identified in low-current rolling-sphere simulations, ensuring robust coverage against direct strikes.

Evaluation of the OCS Protection System of 150 kV Transmission Tower Adjacent to Railway Electrification from Direct Lightning Strikes

Based on the Decree of the Minister of Energy and Mineral Resources Number 55 K/30 / MEM / 2003 concerning the National Transmission Network of the Minister of Energy and Mineral Resources, the following map of the transmission network of Central Java and DIY provinces is presented [17].

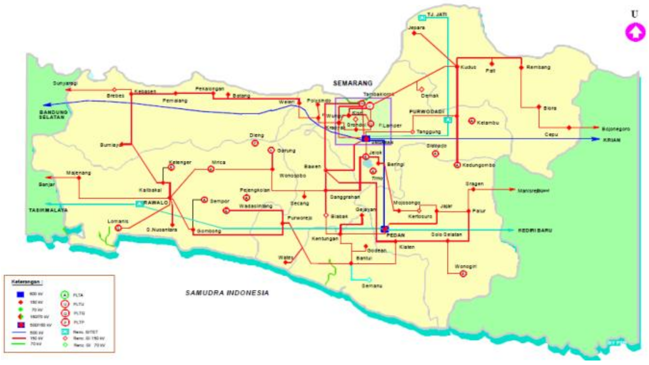

Figure 10. Map of the National Transmission Network of Central Java and Yogyakarta Provinces

Geometric analysis indicated that the closest 150 kV Bantul-Klaten transmission tower sits at a minimum displacement of 94.85 m from the outer rail. Because the absolute maximum calculated lightning strike radius for the OCS is 88.18 m, the rolling sphere modeled around the OCS cannot physically intersect or extend its protection volume to the adjacent grid structures. Consequently, interaction modeling for direct strikes across the two systems is decoupled, requiring independent shielding protocols for each network.

CONCLUSIONS

This study evaluated direct lightning protection coverage for the 1500 V DC Overhead Contact System (OCS) along the Yogyakarta–Solo railway electrification network, comparing the geometric efficacy of the Rolling Sphere Method (RSM) and the Protective Angle Method (PAM) in accordance with IEC 62305. The comparison shows that RSM provides a significantly more accurate and reliable protection zone profile than PAM. By incorporating electrogeometric storm-front curvature under varying lightning peak currents, RSM identifies structural blind spots that linear PAM estimates miss. Across the evaluated network, RSM yields average protection angles of 42.42° on cantilever poles and 56.57° on V-truss beams, compared with PAM's rigid projections of 56.00° and 56.30°, respectively.

Under current physical configurations, both the cantilever poles and V-truss beam structures provide only Level III protection. Given that the corridor experiences severe lightning activity, with more than 60,000 cloud-to-ground flashes annually, this shielding performance is insufficient to meet standard channel protection requirements for vital public transit infrastructure, leaving lower OCS equipment vulnerable to low-current direct strikes. Additionally, geometric modeling of the adjacent 150 kV Bantul–Klaten transmission grid shows a minimum tower separation of 94.85 m from the OCS rail. Because this separation exceeds the maximum calculated OCS striking distance radius of 88.18 m, the rolling sphere volumes of the power grid and railway system cannot intersect, indicating that the two networks are structurally decoupled and require independent shielding protocols.

To achieve target compliance with Level I or Level II protection standards and safeguard operational continuity against lightning-induced back-flashovers, targeted infrastructure upgrades are necessary. Implementing the closed-loop optimization framework established in this study. It will specifically, by

https://doi.org/10.25077/xxxxx

installing dedicated air terminals atop OCS support poles or optimizing inter-pole geometric spacing, eliminate localized exposure risks and ensure long-term system reliability for the Yogyakarta–Solo line.

ACKNOWLEDGMENT

The first author would especially like to thank Mrs. Ir. Riska Sasanti Danartini, S.T., M.Sc., IPP, Head of the Railway Infrastructure Section, and Mr. Bomby Duswara, S.T., PPK of Development Activities Section III of Balai Teknik Perkeretaapian Kelas I Semarang, Directorate General of Railways, Ministry of Transportation, for giving the author the opportunity to conduct research, as well as the various parties who have helped in the completion of this research.

REFERENCES

[1] M. Nakayama *et al.*, “Revision of lightning protection map for overhead contact line system,” *2016 33rd International Conference on Lightning Protection, ICLP 2016*, 2016, doi: 10.1109/ICLP.2016.7791510.

[2] T. Gonen, *Electrical Power Transmission System Engineering*. 2015. doi: 10.1201/b17055.

[3] IEEE Standard for Transient Overvoltage Protection of DC Electrification Systems by Application of DC Surge Arresters, IEEE Std 1653.2-2009 (R2020), 2020, doi: 10.1109/IEEESTD.2009.5354133.

[4] S. V. Spitsa and A. A. Suvorov, "Analysis and calculation of back-flashover rates on high-voltage transmission lines subject to direct lightning strikes," IEEE Trans. Power Deliv., vol. 32, no. 4, pp. 1892–1900, Aug. 2017.

[5] CENELEC Standard EN 50122-1:2011/A4:2022, Railway applications - Fixed installations - Electrical safety, earthing and the return circuit - Part 1: Protective provisions against electric shock, European Committee for Electrotechnical Standardization, Brussels, Belgium, 2022.

[6] IEC Standard 62848-1:2019, Railway applications - Fixed installations - DC surge arresters and voltage limiting devices - Part 1: Metal-oxide surge arresters without gaps, International Electrotechnical Commission, Geneva, Switzerland, 2019.

[7] W. A. Chisholm, “Lightning Protection,” *Electric Power Generation, Transmission, and Distribution: The Electric Power Engineering Handbook*, pp. 18-1-18–14, 2019, doi: 10.1201/9781315222424-18.

[8] A. L. Hartisa, A. Syakur, and M. Facta, “Evaluate Lightning Protection Zone of DC Electric Railway at Solo - Yogyakarta Track Using Rolling Sphere Method,” in *Proceedings - 11th International Conference on Information Technology, Computer and Electrical Engineering, ICITACEE 2024*, Institute of Electrical and Electronics Engineers Inc., 2024, pp. 150–155. doi: 10.1109/ICITACEE62763.2024.10762807.

[9] J. He, R. Zeng, and B. Zhang, "Methodology for evaluating lightning shielding failure of overhead transmission lines and substations," IEEE Trans. Power Deliv., vol. 31, no. 5, pp. 2210–2218, Oct. 2016, doi: 10.1109/TPWRD.2016.2520012.

[10] Y. Kishimoto, “Consideration of protection angle method and lightning protection rules for sides of high-rise buildings in IEC 62305 standard,” *NTT Facilities Research Institue Inc.*, pp. 837–840, 2009.

[11] IEEE Guide for Direct Lightning Stroke Shielding of Substations, IEEE Std 998-2012 (Reaffirmed 2017), IEEE Power and Energy Society, New York, NY, USA, 2017.

[12] IEC Standard 62305-3:2010, Protection against lightning - Part 3: Physical damage to structures and life hazard, International Electrotechnical Commission, Geneva, Switzerland, 2010.

[13] M. E. A., A. M. S., and S. S. M., “Analysis of Lightning Strikes on The Transmission Line by Considering The Frequency-Dependent Model,” *Quantum Journal of Engineering, Science and Technology*, vol. 2, no. 6, pp. 12–36, 2021.

[14] A. De Conti and S. Visacro, "Assessment of lightning shielding performance of overhead lines using advanced electrogeometric formulations," IEEE Trans. Electromagn. Compat., vol. 60, no. 4, pp. 1012–1019, Aug. 2018, doi: 10.1109/TEMC.2017.2764101.

[15] F. A. Uribe, J. L. Naredo, and P. Moreno, "Computation of electromagnetic transients on DC railway overhead contact systems during lightning strikes using ATP-EMTP," Electr. Power Syst. Res., vol. 170, pp. 112–120, May 2019, doi: 10.1016/j.epsr.2019.01.015.

[16] BS EN / IEC 62305-1:2011, Protection against lightning - Part 1: General principles, British Standards Institution / IEC, London, UK, 2018.

[17] World Bank, "Electrification and Transmission Grid Connectivity Assessment Guidelines," Energy & Extractives Global Practice Technical Paper, Washington, DC, USA, 2018.

[18] CIGRE Working Group C4.401, "Lightning Mechanism and Shielding Failure Evaluation of Overhead Lines," CIGRE Technical Brochure 705, Paris, France, Nov. 2017.

[19] F. Fiamingo, M. Marzinotto, and C. A. Nucci, "Lightning transient overvoltages and optimal surge arrester allocation along DC traction overhead lines," IEEE Trans. Transp. Electrif., vol. 6, no. 3, pp. 1145–1154, Sept. 2020, doi: 10.1109/TTE.2020.2995812.

[20] H. K. Hoidalen, A. Ametani, and J. A. Martinez, "Electromagnetic transient simulation of railway electrification systems under extreme impulse current injection," IEEE Trans. Power Deliv., vol. 36, no. 2, pp. 845–854, Apr. 2021, doi: 10.1109/TPWRD.2020.2999120.

NOMENCLATURE

α_{limit}	meaning of setpoint
Σ	meaning of comparator
γ	meaning of security level (meter)
$\alpha°$	meaning of angle of protection (degree)
h	meaning of pole height (meter)
r	meaning of strike distance (meter)
S	meaning of strike distance (meter)
I_p	meaning of lightning current (kA)
l	meaning of lightning current (kA)
h	meaning of pole height (meter)

AUTHOR(S) BIOGRAPHY

Anindira Listy Hartisa, S.T., M.T.

Anindira Listy Hartisa, S.T., M.T., is an associate lecturer in the Department of Electrical Engineering at Universitas Negeri Semarang. She earned a master's degree with *magna cum laude* in Electrical Engineering from Universitas Diponegoro, a bachelor's degree from Universitas Islam Sultan Agung Semarang, and a diploma degree from Politeknik Perkeretaapian Indonesia Madiun, Indonesia. She has 4 years of experience as a

Railway Signaling Analyst, covering signaling, telecommunications, electrical systems, and infrastructure maintenance. Her research interests include Railway Signaling Systems, High Voltage Protection, Energy System Auditing, and Electrical Protection Systems. Committed to inspiring the next generation of engineers through knowledge and experience in electrical engineering and railway systems. She can be reached via email at diraanin@gmail.com and anindiralisty@mail.unnes.ac.id.

Dr. Ir. Abdul Syakur, S.T., M.T., IPU
Dr. Ir. Abdul Syakur, S.T., M.T., IPU is a senior lecturer in the Electrical Engineering Department at Universitas Diponegoro, Semarang, Indonesia. He received his doctoral, master's, and bachelor's degrees in electrical engineering from Universitas Diponegoro, Institut Teknologi Bandung, and Universitas Gadjah Mada, in 1997, 2002, and 2015, respectively. He has been an Associate Professor at Universitas Diponegoro, Semarang, Indonesia, since 2007. He is currently the head of the High-Voltage Innovation and Technology (Hi-VIT) research laboratory and has been a member of IEEE since 2011. His research interests include high-voltage generation, high-voltage insulation technology, electrical tracking in insulator materials, partial discharge, lightning phenomena, and lightning protection systems. He can be contacted at gakusei2003@yahoo.com and syakur@elektro.undip.ac.id.

Ir. Mochammad Facta, S.T., M.T., Ph.D.
Ir. Mochammad Facta, S.T., M.T., Ph.D. is currently an Associate Professor in the Electrical Engineering Department at Universitas He has served as the chair of the master's program in electrical engineering at Universitas Diponegoro. He received his Ph.D. in electrical engineering from Universiti Teknologi Malaysia, a master's degree with cum laude from Institut Teknologi 10 Nopember Surabaya, Indonesia, and a bachelor's degree from Universitas Hasanuddin, Makassar, Indonesia. He was awarded professional engineering status by Universitas Diponegoro in association with the Indonesian Engineer Association (PII). His research interests include electrical energy conversion, power electronics drives, power systems, and high-voltage applications. He can be contacted at mochfacta@gmail.com and facta@elektro.undip.ac.id.

Dr. Nur Iksan, S.T., M.Kom.
Dr. Nur Iksan, S.T., M.Kom., was born in Grobogan, Indonesia, on March 7, 1983. He has been a lecturer at Semarang State University, Indonesia, since 2012. He received his doctoral degree in electrical engineering from Universitas Diponegoro, a master's degree in informatics engineering from Universitas Dian Nuswantoro, Indonesia, and a bachelor's degree from Universitas Negeri Semarang, Indonesia. He is actively engaged in research and writes articles for scientific publications on artificial intelligence, with a focus on energy management in smart grids. He is an active member of professional organizations, including the IEEE. He can be contacted at nur.iksan@mail.unnes.ac.id.

APPENDICES

Based on the results of lightning activity records from January to December 2019 with a buffer radius of 2 km from the tower, there were 1314 lightning events on the 150 kV Bantul-Klaten conductor. Based on the suitability of the location with the test location at Brambanan Station, the data on lightning activity across Bantul-Klaten is as follows.

Table 6. Lightning Activity Across Bantul - Klaten

Tower	Lightning Type					
	Lightning (-)			Lightning (+)		
	Amount of Lightning (-)	Avg Lightning Peak Current (-)	(kA)	Amount of Lightning (+)	Avg Lightning Peak Current (+)	(kA)
	a	b	a×b	c	d	c×d
5	94	-18.0638	-1698	8	40.125	321
6	97	-16.9175	-1641	7	28.2857	198
13	98	-17.7347	-1738	10	16.9	169
14	103	-18.5922	-1915	10	22.4	224
15	112	-19.0357	-2132	10	22.4	224
16	111	-18.5586	-2060	12	17.75	213
17	110	-18	-1980	12	17.6667	212
18	106	-17.3302	-1837	9	18.2222	164
19	95	-16.4737	-1565	8	17.25	138
45	100	-15.39	-1539	9	18.7778	169
46	107	-16.5327	-1769	11	17	187
47	106	-18.2264	-1932	12	14.25	171
48	111	-16.6757	-1851	12	20	240
49	107	-16.3458	-1749	9	23.6667	213
50	99	-16.6667	-1650	9	24.2222	218
62	103	-13.6796	-1409	6	11.3333	68
63	113	-14.3717	-1624	6	11.3333	68
64	116	-14.431	-1674	8	9.875	79
65	117	-14.1624	-1657	9	9.4444	85
66	120	-13.6917	-1643	10	11.4	114
67	149	-13.8658	-2066	12	10.0833	121
68	149	-14.4631	-2155	13	13.0769	170
69	166	-14.994	-2489	11	10.7273	118
70	186	-14.9247	-2776	11	11.3636	125
71	202	-14.8614	-3002	11	11.5455	127
72	193	-14.6425	-2826	14	11	154
73	197	-14.665	-2889	16	12.3125	197
74	184	-15.2717	-2810	16	11.0625	177
75	175	-14.9543	-2617	16	15.875	254
76	159	-14.43	-2294.0043	12	15.3333	184
77	137	-14.4015	-1973	14	16.7857	235
78	143	-14.3357	-2050	19	13.6842	259.9998
79	129	-13.093	-1689	17	14.1765	241
80	121	-11.5455	-1397	17	12.7059	216
81	123	-11.0488	-1359	18	14.5	261
82	138	-12.0507	-1663	16	15.5625	249
83	144	-13.0625	-1881	16	14.9375	239
84	144	-12.8958	-1857	18	13.7222	247
85	133	-12.3384	-1641	19	14.1579	269
085A	133	-12.3534	-1643	18	12.5	225

https://doi.org/10.25077/xxxxx

Tower	Lightning Type					
	Lightning (-)			Lightning (+)		
	Amount of Lightning (-)	Avg Lightning Peak Current (-)	(kA)	Amount of Lightning (+)	Avg Lightning Peak Current (+)	(kA)
	a	b	a×b	c	d	c×d
Total Amount of Lightning (-/+)	**5230**			**491**		
Total (-/+)			**-78140**			**7544**